Arabian Journal of Chemistry (2019) 12, 3890–3901

King Saud University

Arabian Journal of Chemistry

www.ksu.edu.sa
www.sciencedirect.com

ORIGINAL ARTICLE

Structure and cytotoxic activity of terpenoid-like chalcones

Rosa S. Lima [a], Caridad N. Perez [a], Cameron C. da Silva [a], Mabio J. Santana [a], Luiz H.K. Queiroz Júnior [a], Stefânio Barreto [b], Manoel O. de Moraes [b], Felipe T. Martins [a,*]

[a] *Chemical Institute, Federal University of Goiás, Campus Samambaia, CP 131, Goiânia, GO 74001-970, Brazil*
[b] *Department of Physiology and Pharmacology, Federal University of Ceará, Fortaleza, CE 3157, Brazil*

Received 21 December 2015; accepted 23 February 2016
Available online 3 March 2016

KEYWORDS

Claisen–Schmidt condensation;
Crystal structure;
X-ray diffraction;
Cytotoxic activity;
Antitumor compounds

Abstract Compounds with either ionone or chalcone skeletons present many biological properties including anticancer activity. Here we have prepared eight terpenoid-like chalcones in order to assess whether hybrid compounds with both structural frameworks could exhibit enhanced pharmacological profile. The terpenoid-like chalcones were synthesized by means of Claisen–Schmidt condensation reaction, using either α- or β-ionone with substituted benzaldehydes. The structure of six derivatives was elucidated by single crystal X-ray diffraction technique for the first time. Cyclohexene ring adopts half-chair conformation in α-ionone-derived chalcone with quaternary carbon at the flap, while twist puckering was observed in β-ionone terpenoid-like chalcones. All prepared compounds were tested for their cytotoxic activity against three cancer cell lines, namely SF-295, HCT-116 and OVCAR-8, which allowed us to establish some structure–activity relationships. Terpenoid-like chalcones with nitro substituted phenyl rings, regardless of its position and ionone type, were the most active chalcones among all that tested. The IC_{50} values do also reveal a trend of decrease in cytotoxic activity with weak electron-withdrawing groups at phenyl ring.

1. Introduction

Chalcones and their derivatives have a great pharmaceutical relevance (Bukhari et al., 2012) due the fact that they are used as ameliorative (Sarojini et al., 2011), inhibitors of nitric oxide production, cytotoxic agents (Reddy et al., 2012), antimicrobial (Asiri and Khan, 2011; Bukhari et al., 2013a), anti-inflammatory (Bukhari et al., 2013b, 2014b, 2015; Jantan et al., 2014), anticancer (Modzelewska et al., 2006), antimalarial (Srivastava et al., 2008), antiviral agents and UV radiation protectors (Raj et al., 2012).

* Corresponding author. Tel.: +55 62 3521 1097; fax: +55 62 3521 1167.
E-mail address: felipe@ufg.br (F.T. Martins).
Peer review under responsibility of King Saud University.

ELSEVIER Production and hosting by Elsevier

http://dx.doi.org/10.1016/j.arabjc.2016.02.013

Compounds with the trimethylcyclohexene moiety are responsible for the aroma of essential oils and therefore they have attracted attention of fragrance and flavor industries. Among these compounds, ionones and their derivatives are raw materials for synthesis of many natural products and intermediates in the metabolism of terpenoids (for instance, in the carotenoid biosynthesis). In addition, these compounds have been isolated from many natural sources (Lutz-Wall et al., 1998). Furthermore, derivatives of ionones (e.g., 3-hydroxy-β-ionone) are valuable intermediates for the chemical-enzymatic synthesis of carotenoids such as astaxanthin and zeaxanthin (Markovich et al., 1998). β-ionone is used as starting material in the synthesis of vitamin A (retinol). Additionally, some ionone derivatives have shown several biological activities (Raynaud et al., 2006; Chandra et al., 2006; Suryawanshi et al., 2007). As an example, we can cite an aryl-substituted pyrimidine terpenoid-like derivative with leishmanicidal activity (Chandra et al., 2006).

Structurally, chalcones have the same pharmacophore found in flavones and isoflavones, which are potent inhibitors of DNA topoisomerase II and therefore are considered as potent antitumor and anti-HIV agents (Wang et al., 1997). Recently, chalcone analogs with three substituted aromatic rings have demonstrated potent NO and reactive oxygen species (ROS) production inhibition and cytotoxic properties (Bukhari et al., 2014c; Reddy et al., 2012).

Based on the known biological properties of compounds with either ionone or chalcone skeletons, including anticancer activity, we have prepared eight terpenoid-like chalcones in order to assess whether hybrid compounds with both structural frameworks could exhibit enhanced pharmacological profile due to synergism between them. The terpenoid-like chalcones were synthesized by mean of Claisen–Schmidt condensation reaction, using either α- or β-ionone with substituted benzaldehydes (Findik et al., 2009), as shown in Scheme 1, and their structures were doubtless elucidated by single crystal X-ray diffraction technique besides complementary methodologies such as NMR. At last, all prepared compounds were tested for their cytotoxic activity against three cancer cell lines, namely SF-295 (central nervous system), HCT-116 (colon) and OVCAR-8 (breast cancer), which allowed us to establish some structure–activity relationships.

2. Experimental

2.1. General procedure for synthesis of terpenoid-like chalcones 1–8

α-Ionone, β-ionone, and benzaldehyde derivatives were highest reagent grade commercial products. A water solution of sodium hydroxide (0.123 g) was added to mixture of ionone (1.5 mmol) and benzaldehyde derivative (2.5 mmol) in methanol (10 ml). The reaction mixture was stirred at room temperature for 12 h. At the end of reaction time, the mixture was diluted with CH_2Cl_2, treated with HCl solution (10%), and washed with water. The organic phase was dried over anhydrous Na_2SO_4 and filtered. The solvent was slowly evaporated and the crystals suitable for structure determination were isolated without further crystallization. Furthermore, the product of the reaction was chromatographed on a silica gel column, 120–230 mesh, and eluted with ethyl acetate: hexane (2:8).

2.2. Structure determination by single-crystal X-ray diffraction technique

Suitably shaped single crystals of 1, 3–8 were selected for the X-ray diffraction data collection on a Bruker-AXS Kappa Duo diffractometer with an APEX II CCD detector. Even though compound 5 has been determined previously (Zou et al., 2012), we performed the collection of its single-crystal X-ray data. Therefore, all geometrical parameters of 5 presented here are from our structure redetermination. We have deposited crystal data of 5 with Cambridge Crystallographic Data Centre (CCDC) under deposit code 1029769. Compound 2 was not redetermined in this study and its crystal data are from the literature (CCDC deposit code 818053) (Fernandes et al., 2013). Mo Kα radiation from an IμS microsource with multilayer optics was employed. Diffraction images were recorded by φ and ω scans set using APEX2 software (Bruker, 2012). This software was also employed to treat the raw dataset for indexing, integrating, reducing and scaling of the reflections. Next, the crystallographic softwares were used as follows: SIR2004 (structure solving) (Burla et al., 2005), SHELXL-97 (structure refinement) (Sheldrick, 2008), MERCURY and ORTEP-3 (structure analysis and representations) (Macrae et al., 2008; Farrugia, 1997). All structures were solved through identification of all non-hydrogen atoms in asymmetric units directly from the Fourier synthesis of the structure factors after retrieval of their phase using the direct methods. Each initial model was refined by full-matrix least squares method on F^2, adopting free anisotropic and constrained isotropic atomic displacement parameters for non-hydrogen and hydrogen atoms, respectively. In the case of hydrogens, their U_{iso} was set to either $1.2U_{eq}$ of the bonded carbon, except for methyl hydrogens in which their U_{iso} was set to $1.5U_{eq}$ of the corresponding carbon. Hydrogen coordinates were stereochemically defined and constrained in the refinements, oscillating as that of the bonded carbon to keep idealized bond angles and lengths fixed in 0.93 Å (C^2_{sp}—H), 0.96 Å (C^3_{sp}—H in CH_3 groups), 0.97 Å (C^3_{sp}—H in CH_2 groups), and 0.98 Å (C^3_{sp}—H in CH groups).

Compounds 5–8 were present with two twist conformations of the cyclohex-1-ene ring. This conformational variability has occurred due to static disorder into the six-membered ring. The static disorder was modeled by splitting the CH_2 carbons and hydrogens over two sites with occupancy factors constrained to the following values: 50% (both conformations of 6), 55% (major conformation of 5 and 7 whose carbon fractions were labeled as C14—C16), 65% (major conformation of 8 whose carbon fractions were labeled as C14—C16), 45% (minor conformation of 5 and 7 whose carbon fractions were labeled as C14′—C16′), or 35% (minor conformation of 8 whose carbon fractions were labeled as C14′—C16′). It is important to state that all site occupancy factors (SOFs) of these carbons were refined freely in trial refinements. The SOFs found from initial refinements were then constrained to the corresponding sites and in sequence hydrogens were stereochemically positioned using a riding model on carbon as described above. Such refinement procedure has resulted in better *R*-factors, the lowest residual electronic density in the unit cell and refinement convergence. It is striking to note that unusual values of *R*-factors were outputted from refinement of 1 and 3, which could be a consequence of a static disorder due to different cyclohex-2-ene ring puckering modes similar to those modeled reliably for terpenoid-like chalcones 5–8. In trial refinements constraining the primary site occupancy of cyclohex-2-ene carbon atoms to 50%, extra occupancy sites were observed but they were very close together with the primary ones. In attempt to refine them as carbon fractions, high correlation between all tested SOFs and atomic displacement parameters was observed applying the classical split-atom

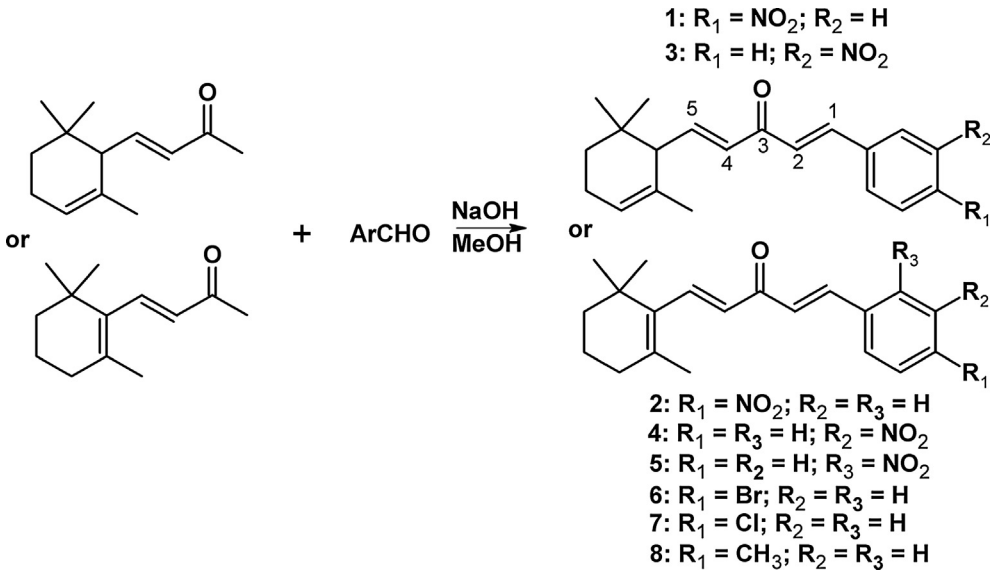

Scheme 1 General scheme for synthesis of terpenoid-like chalcones studied here. Compounds 2 and 5 have been previously synthesized and featured (Zou et al., 2012; Fernandes et al., 2013).

approach to the structural model of 1 and 3, as well as refinements were unstable without convergence. Therefore, we have used the classical harmonic model based upon a development of the atomic displacement parameters with just one site instead of the split-position model.

2.3. Additional characterization

Other characterizations of synthesized compounds were performed as follows. Melting points were measured in a Micro Química MQAPF-301 apparatus. The infrared spectra were obtained in Bomem M102 Fourier Transform spectrometer. Samples were analyzed by the FTIR transmission technique as KBr pellets (mixtures comprising 200 mg of KBr and 1 mg of sample). NMR spectra were recorded on a Bruker Avance III, operating at 500.13 MHz for ^{1}H and 125.77 MHz for ^{13}C, equipped with a 5 mm TBI probe (^{1}H, ^{13}C and XBB).

2.3.1. (1E,4E)-1-(4-nitrophenyl)-5-(2,6,6-trimethylcyclohex-2-en-1-yl)penta-1,4-dien-3-one

(**1**): Orange solid, 70% yield, mp 104–106 °C. IR ν_{max} 2944–2822, 1668, 1605, 1518, 1435, 1342, 1278, 1211, 1186, 1113, 980, 856, 814, 757, 682. ^{1}H NMR [500 MHz, δ (ppm), DMSO-d6]: 8.25 (*d*, 8.7 Hz, H-3/5), 8.06 (*d*, 8.7 Hz, H-2/6), 7.70 (*d*, 15.8 Hz, H-7), 7.56 (*d*, 15.8 Hz, H-8), 6.92 (*dd*, 15.4; 9.7 Hz, H-11), 6.45 (*d*, 15.4 Hz, H-10), 5.52 (*br s*, H-16), 2.40 (*d*, 9.7 Hz, H-12), 2.04 (*m*, H-15), 1.55 (*m*, H-14a), 1.20 (*m*, H-14b), 1.56 (*br d*, H-20), 0.91 (*s*, H-18), 0.83 (*s*, H-19). ^{13}C NMR [125 MHz, δ (ppm), DMSO-d6]: 187.6 (C-9), 149.2 (C-11), 147.8 (C-4), 141.2 (C-1), 139.7 (C-7), 131.6 (C-17), 130.8 (C-10), 129.6 (C-2/6), 127.8 (C-8), 123.7 (C-3/5), 122.0 (C-16), 53.9 (C-12), 32.5 (C-13), 30.4 (C-14), 27.5 (C-19), 26.3 (C-18), 22.6 (C-15), 22.4 (C-20).

2.3.2. (1E,4E)-1-(4-nitrophenyl)-5-(2,6,6-trimethylcyclohex-1-en-1-yl)penta-1,4-dien-3-one

(**2**): Orange solid, 78% yield, mp 134–135 °C. IR ν_{max} 2923, 1663, 1615, 1591, 1512, 1454, 1416, 1343, 1247, 1198, 1144, 1090, 981, 861, 752, 716, 620. ^{1}H NMR [500 MHz, δ (ppm), DMSO-d6]: 8.27 (*d*, 8.6 Hz, H-3/5), 8.05 (*d*, 8.6 Hz, H-2/6), 7.73 (*d*, 16.0 Hz, H-7), 7.52 (*d*, 16.0 Hz, H-11), 7.50 (*d*, 16.0 Hz, H-8), 6.59 (*d*, 16.0 Hz, H-10), 2.11 (*m*, H-16), 1.80 (*s*, H-20), 1.60 (*m*, H-15), 1.47 (*m*, H-14), 1.10 (*s*, H-18/19). ^{13}C NMR [125 MHz, δ (ppm), DMSO-d6]: 188.0 (C-9), 147.9 (C-4), 142.4 (C-7), 141.3 (C-1), 139.3 (C-11), 137.4 (C-17), 135.9 (C-12), 129.5 (C-6/8), 129.5 (C-2), 129.3 (C-10), 123.8 (C-3/5), 39.4 (C-14), 33.7 (C-13), 33.2 (C-16), 28.5 (C-18/19), 21.5 (C-20), 18.3 (C-15).

2.3.3. (1E,4E)-1-(3-nitrophenyl)-5-(2,6,6-trimethylcyclohex-2-en-1-yl)penta-1,4-dien-3-one

(**3**): Yellow solid, 80% yield, mp 90–92 °C. IR ν_{max} 3090–2860, 1658, 1604, 1524, 1471, 1438,1353, 1283, 1252, 1209, 1134, 1092, 995, 947, 883, 829, 744, 696, 670, 578. ^{1}H NMR [500 MHz, δ (ppm), DMSO-d6]: 8.63 (*br t*, 2.0 Hz, H-6), 8.26 (*m*, H-4), 8.25 (*m*, H-2), 7.77 (*d*, 15.9 Hz, H-7), 7.73 (*t*, 7.9 Hz, H-3), 7.57 (*d*, 15.9 Hz, H-8), 6.92 (*dd*, 15.4; 9.7 Hz, H-11), 6.47 (*dd*, 15.4; 0.6 Hz, H-10), 5.53 (*br s*, H-16), 2.41 (*d*, 9.7 Hz, H-12), 2.05 (*m*, H-15), 1.57 (*m*, H-14a), 1.22 (*m*, H-14b), 1.58 (*br d*, H-20), 0.92 (*s*, H-18), 0.85 (*s*, H-19). ^{13}C NMR [125 MHz, δ (ppm), DMSO-d6]: 188.1 (C-9), 149.0 (C-11), 148.4 (C-5), 140.0 (C-7), 136.6 (C-1), 134.6 (C-2), 131.8 (C-17), 131.0 (C-10), 130.6 (C-3), 127.0 (C-8), 124.5 (C-4), 123.0 (C-6), 122.3 (C-16), 53.9 (C-12), 32.1 (C-13), 30.7 (C-14), 27.6 (C-19), 26.6 (C-18), 22.6 (C-15), 22.5 (C-20).

2.3.4. (1E,4E)-1-(3-nitrophenyl)-5-(2,6,6-trimethylcyclohex-1-en-1-yl)penta-1,4-dien-3-one

(**4**): Yellow solid, 90% yield, mp 133–135 °C. IR ν_{max} 3090–2863, 1662, 1596, 1536, 1457, 1349, 1307, 1205, 1168, 1096, 1030, 987, 921, 885, 818, 734, 691, 661, 565. ^{1}H NMR [500 MHz, δ (ppm), DMSO-d6]: 8.62 (*br t*, 1.8 Hz, H-6), 8.24 (*m*, H-4), 8.23 (*m*, H-2), 7.77 (*d*, 16.0 Hz, H-7), 7.72 (*t*, 7.8 Hz, H-3), 7.51 (*d*, 16.0 Hz, H-8), 7.49 (*d*, 16.0 Hz, H-11), 6.61 (*d*, 16.0 Hz, H-10), 2.10 (*m*, H-16), 1.81 (*s*, H-20), 1.59 (*m*, H-15), 1.47 (*m*, H-14), 1.10 (*s*, H-18/19). ^{13}C NMR

[125 MHz, δ (ppm), DMSO-d6]: 188.0 (C-9), 148.1 (C-5), 142.2 (C-11), 139.6 (C-7), 137.5 (C-17), 136.6 (C-1), 135.9 (C-12), 134.4 (C-2), 130.2 (C-3), 129.1 (C-10), 128.4 (C-8), 124.3 (C-4), 122.9 (C-6), 39.2 (C-14), 33.5 (C-13), 33.1 (C-16), 28.5 (C-18/19), 21.4 (C-20), 18.3 (C-15).

2.3.5. (1E,4E)-1-(2-nitrophenyl)-5-(2,6,6-trimethylcyclohex-1-en-1-yl)penta-1,4-dien-3-one

(**5**): Orange solid, 85% yield, mp 130–132 °C. IR ν_{max} 3098–2808, 1671, 1607, 1573, 1526, 1451, 1352, 1323, 1300, 1271, 1207, 1143, 1091, 981, 906, 865, 795, 749, 708, 639, 569. ^{1}H NMR [500 MHz, δ (ppm), DMSO-d6]: 8.06 (*dd*, 8.1; 1.2 Hz, H-5), 8.02 (*dd*, 7.8; 1.2 Hz, H-2), 7.88 (*d*, 16.0 Hz, H-7), 7.80 (*t*, 7.8 Hz, H-3), 7.67 (*t*, 8.0 Hz, H-4), 7.50 (*d*, 16.0 Hz, H-11), 7.31 (*d*, 16.0 Hz, H-8), 6.54 (*d*, 16.0 Hz, H-10), 2.10 (*m*, H-16), 1.81 (*s*, H-20), 1.59 (*m*, H-15), 1.46 (*m*, H-14), 1.10 (*s*, H-18/19). ^{13}C NMR [125 MHz, δ (ppm), DMSO-d6]: 188.0 (C-9), 148.6 (C-6), 143.2 (C-11), 137.6 (C-17), 136.8 (C-7), 135.7 (C-12), 133.9 (C-3), 133.7 (C-1), 130.2 (C-4), 129.7 (C-8), 129.6 (C-10), 129.1 (C-2), 124.8 (C-5), 39.4 (C-14), 33.5 (C-13), 32.8 (C-16), 28.4 (C-18/19), 21.4 (C-20), 18.1 (C-15).

2.3.6. (1E,4E)-1-(4-bromophenyl)-5-(2,6,6-trimethylcyclohex-1-en-1-yl)penta-1,4-dien-3-one

(**6**): Yellow solid, 76% yield, mp 96–98 °C. IR ν_{max} 3080–2854, 1665, 1601, 1555, 1492, 1457, 1405, 1353, 1324, 1272, 1197, 1058, 995, 891, 844, 816, 717, 660, 585, 527, 492. ^{1}H NMR [500 MHz, δ (ppm), DMSO-d6]: 7.73 (*d*, 8.3 Hz, H-3/5), 7.63 (*d*, 8.3 Hz, H-2/6), 7.61 (*d*, 15.8 Hz, H-7), 7.44 (*d*, 15.8 Hz, H-11), 7.34 (*d*, 15.8 Hz, H-8), 6.55 (*d*, 15.8 Hz, H-10), 2.09 (*br t*, H-16), 1.79 (*s*, H-20), 1.60 (*m*, H-15), 1.47 (*m*, H-14), 1.09 (*s*, H-18/19). ^{13}C NMR [125 MHz, δ (ppm), DMSO-d6]: 188.1 (C-9), 141.8 (C-7), 140.8 (C-11), 136.7 (C-17), 136.0 (C-12), 134.0 (C-1), 131.8 (C-3/5), 130.4 (C-2/6), 129.5 (C-8), 126.5 (C-10), 123.6 (C-4), 39.4 (C-14), 33.7 (C-13), 33.1 (C-16), 28.6 (C-18/19), 21.5 (C-20), 18.4 (C-15).

2.3.7. (1E,4E)-1-(4-chlorophenyl)-5-(2,6,6-trimethylcyclohex-1-en-1-yl)penta-1,4-dien-3-one

(**7**): Orange solid, 78% yield, mp 100–102 °C. IR ν_{max} 2969–2871, 1654, 1603, 1494, 1447, 1402, 1321, 1194, 1085, 1016, 976, 884, 815, 781, 683, 631, 573, 499. ^{1}H NMR [500 MHz, δ (ppm), DMSO-d6]: 7.81 (*d*, 8.7 Hz, H-2/6), 7.50 (*d*, 8.7 Hz, H-3/5), 7.63 (*d*, 16.3 Hz, H-7), 7.44 (*d*, 16.3 Hz, H-11), 7.32 (*d*, 16.3 Hz, H-8), 6.55 (*d*, 16.3 Hz, H-10), 2.09 (*br t*, H-16), 1.79 (*s*, H-20), 1.59 (*m*, H-15), 1.47 (*m*, H-14), 1.09 (*s*, H-18/19). ^{13}C NMR [125 MHz, δ (ppm), DMSO-d6]: 188.8 (C-9), 142.5 (C-7), 141.4 (C-11), 137.4 (C-17), 136.7 (C-12), 135.5 (C-1), 134.4 (C-4), 131.0 (C-2/6), 130.2 (C-8), 129.6 (C-3/5), 127.2 (C-10), 40.1 (C-14), 34.5 (C-13), 33.9 (C-16), 29.3 (C-18/19), 22.3 (C-20), 19.1 (C-15).

2.3.8. (1E,4E)-1-(4-methylphenyl)-5-(2,6,6-trimethylcyclohex-1-en-1-yl)penta-1,4-dien-3-one

(**8**): Yellow solid, 68% yield, mp 92–94 °C. IR ν_{max}. ^{1}H NMR [500 MHz, δ (ppm), DMSO-d6]: 7.66 (*d*, 8.8 Hz, H-2/6), 7.62 (*d*, 16.0 Hz, H-7), 7.41 (*d*, 16.0 Hz, H-11), 7.25 (*d*, 8.8 Hz, H-3/5), 7.23 (*d*, 16.0 Hz, H-8), 6.56 (*d*, 16.0 Hz, H-10), 2.09 (*m*, H-16), 1.79 (*s*, H-20), 1.59 (*m*, H-15), 1.47 (*m*, H-14), 1.09 (*s*, H-18/19). ^{13}C NMR [125 MHz, δ (ppm), DMSO-d6]: 188.1 (C-9), 142.2 (C-7), 141.3 (C-11), 140.4 (C-4), 136.3 (C-17), 135.9 (C-12), 132.0 (C-1), 129.5 (C-8), 129.5 (C-2/6), 128.5 (C-3/5), 124.9 (C-10), 39.4 (C-14), 33.7 (C-13), 33.1 (C-16), 28.6 (C-18/19), 21.0 (C-20), 18.4 (C-15).

2.4. Cytotoxicity assay

Terpenoid-like chalcones were tested for cytotoxicity against three tumor cell lines: SF-295 (central nervous system), HCT-116 (colon cancer) and OVCAR-8 (breast cancer). All cell lines were obtained from National Cancer Institute (NCI) (Skehan et al., 1990) and they are the first choice cancer cell lines used for the cytotoxicity screening in the Laboratório de Oncologia from Universidade Federal of Ceará, where the assays were performed. These cancer cell lines were cultivated in RPMI 1640 medium supplemented with fetal bovine serum (10%), glutamine (2 mm), penicillin (100 U/ml), and streptomycin (100 mg/ml), at 37 °C, with CO_2 (5%). The MTT assay was used for the cytotoxicity evaluation of terpenoid-like chalcones (Berridge et al., 1996; Mossman, 1983). Cells were plated at a concentration of 0.1×10^6 cells/ml for strains SF-295 and OVCAR-8-3 and 0.7×10^5 cells/ml for the HCT-116 strain.. Doxorubicin (5 μg/ml) and DMSO (0.05%) were used as positive and negative controls, respectively. After 24 h, the terpenoid-like chalcones were added to the wells to obtain the final concentration (25 μg/ml). After 72 h, plates were centrifuged (1500 rpm, 15 min), and the supernatants were removed. An aliquot (150 μl) from the MTT soln. (0.5 mg/ml) was added into each well, and the plates were incubated for 3 h under the same conditions described above. Then, DMSO (150 μl) was poured to dissolve the precipitate, and the absorbance was measured at 595 nm. This experiment was run in three replicates, and all absorbance values were converted into a cell growth inhibition percentage (GI-%) by the following equation: $GI\text{-}\% = 100 - [(T/C) \times 100\%]$. C is the absorbance for the negative control, and T was the absorbance in the presence of the tested extract. Those compounds that presented more than 85% of activity were selected to be tested at concentrations varying from 0.078 to 5 μg/ml to determine IC_{50} values by nonlinear regression using GraphPad Prism 4.0 software.

3. Results and discussion

3.1. Conformational analysis from crystal structures

The terpenoid-like chalcones 1–8 were synthetized by Claisen–Schmidt condensation reaction between α- and β-ionone with substituted benzaldehydes dissolved in methanol (MeOH). The reactions were catalyzed by sodium hydroxide (NaOH) in aqueous solution at room temperature for 12 h. The structure of all compounds is presented in Scheme 1. All products were characterized by melting point, infrared and NMR spectroscopy, and single-crystal X-ray diffraction technique. Except for compounds 2 and 5, their crystal structure is reported for the first time here. In addition, we have also redetermined the structure of 5 in this study. Such structure redetermination allowed us to know correctly the population of each cyclohexene twist conformation. Zou et al. (2012) have

wrongly modeled the disordered methylene groups of cyclohexene over two sets of sites with occupancy ratios of 0.50:0.50 and 0.60:0.40. This does result obligatorily in an unexpected planar cyclohexene conformation of 10% occupancy in addition to the two expected twist conformations. Furthermore, an extremely short C^3_{sp}—C^3_{sp} bond length is observed in this planar conformation (according to Zou et al. (2012) atom labeling scheme, C15—C16′ measures 1.21 Å). Therefore, our redetermination does correct the previous model to only two twist conformations of the cyclohexene ring with either 55% or 45% occupancy. In our model, all bond lengths into cyclohexene ring are also in agreement with the expected values.

Here, structures of six terpenoid-like chalcones (1, 3, 4, 6–8) have been elucidated by single-crystal X-ray diffraction technique for the first time, while analogs 2 and 5 were already determined crystallographically (Zou et al., 2012; Fernandes et al., 2013) but their crystal data will be also presented here for comparison purposes. Terpenoid-like chalcones 1–5 and 8 crystallized in centrosymmetric space groups as expected from either the absence of chiral centers in their molecular backbones (compounds 2, 4, 5 and 8) or achiral synthesis (compounds 1 and 3) (Table 1). Even without molecular chirality, compounds 6 and 7 were solved in a noncentrosymmetric space group as a consequence of frozen-in chirality upon crystallization, i.e., just one conformation is assumed in the crystal lattice.

The asymmetric unit of all terpenoid-like chalcones is composed by just one molecule, even though cyclohexene ring can adopt two puckering modes in a same structure which resulted in disordered occupancy sites (Fig. 1).

As can be viewed in Fig. 1, a 30% probability ellipsoids representation of the asymmetric units determined in this study, the stereochemistry around both C7═C8 and C10═C11 double bonds is unambiguously assigned as an (*E*)-configuration. In compounds 2, 4–8, all derived from β-ionone, another double bond was clearly identified between C12 and C17 carbons, while in compounds 1 and 3, both derived from α-ionone, C12 is sp^3-hybridized and the cyclohexene double bond does occur between C16 and C17 carbons.

Cyclohexene ring adopts half-chair and twist conformations in chalcones. Half-chair puckering is found in 1 and 3, with C13 deviated by 0.598(7) Å and 0.486(4) Å from the least-squares plane calculated through the other five cyclic coplanar atoms (r.m.s.d. of the C12—C17—C16—C15—C14 fitted atoms is 0.0617 Å in 1 and 0.0889 Å in 3). However, C13 is on the same side of C11 if the cyclohexene mean plane of 1 is taken as reference, while these atoms are on opposite sides relative to the corresponding plane of 3. This conformational feature can be related to the equatorial position of C11 in 1 and the axial one in 3 (see Fig. 1).

Just one twist conformation is observed in 4, with C14 and C15 carbons deviating from the mean plane formed through the C13—C12—C17—C16 atoms by −0.256(3) Å and 0.455(3) Å, respectively (r.m.s.d. of the fitted atoms is 0.0293 Å). This twist conformation was also reported for the conformation with minor occupancy of 2 (C14 and C15 deviations of 0.305 (18) Å and −0.170(12) Å, r.m.s.d. of the fitted coplanar atoms is 0.0668 Å). The other conformation was present with a half-chair puckering with C15 at the flap (C15 deviation of −0.467(13) Å, r.m.s.d. of the fitted coplanar atoms is 0.0384 Å).

Similar to 4, cyclohexene ring of compounds 5–8 does assume twist conformations with C14 and C15 carbons away from the other four coplanar atoms. However, there are two twist conformations featured by flipping C14 and C15 carbons in the last four terpenoid-like chalcones. In 6, C14 and C15 carbons are deviated by 0.276(13) Å and −0.501(12) Å from the mean plane formed through the C13—C12—C17—C16 atoms (r.m.s.d. of the fitted atoms is 0.0116 Å) in one twist conformation, and by −0.321(12) Å and 0.486(10) Å in another one (r.m.s.d. of the C13—C12—C17—C16' fitted atoms is 0.0020 Å). Both twist conformations are equally distributed over the crystal of 6, i.e., site occupancy factors of 50% resulted in the best refinement statistics. On contrary, the major populations of 5 and 7 (both with 55% occupancy) and 8 (65%) are present with a twist conformation featured by C14 and C15 deviating 0.412(7) Å and −0.436(9) Å in 5, 0.35(2) Å and −0.558(11) Å in 7, and 0.325(11) Å and −0.443(11) Å in 8 from the least-square mean plane passing through the four coplanar atoms (r.m.s.d. of the fitted atoms is 0.0209 Å in 5, 0.0177 Å in 7 and 0.0513 Å in 8). In the twist conformation with minor occupancy of either 45% in 5 and 7 or 35% in 8, those respective carbons do deviate −0.447(9) Å and 0.412(11) Å in 5, −0.247(17) Å and 0.425(10) Å in 7, and −0.39(2) Å and 0.45(2) Å in 8 from the least-square mean plane (r.m.s.d. of the fitted atoms is 0.0208 Å in 5, 0.0204 Å in 7 and 0.0179 Å in 8).

Endocyclic torsion angles also describe the cyclohexene conformations observed in terpenoid-like chalcones (Table 2). The lowest dihedral angles within the cyclohexene are those on the C15—C16 and C16—C17 bonds in the C13-flap half-chair conformation of 1 and 3 (torsions C14—C15—C16—C17 and C12—C17—C16—C15). For the C15-flap half-chair conformation of 2, the lowest dihedral angles into cyclohexene are those on the C12—C13 and C12—C17 bonds (torsions C17—C12—C13—C14 and C16—C17—C12—C13). Likewise, the lowest endocyclic cyclohexene torsion angle is on the C12—C17 bond in the twist conformation observed in 2, 4–8 (torsion C13—C12—C17—C16).

Another difference between the molecular conformations of terpenoid-like chalcones resides in the C11—C12 bond axis rotation, resulting in different orientations for cyclohexene rings relative to core carbonyl and olefin moieties. In chalcones 1 and 3 came from α-ionone, the cyclohexene mean plane, calculated through coplanar carbon atoms, does form an angle of ca. 90° [79.7(2)° in 1 and 84.14(14)° in 3] with the least-squares mean plane encompassing carbonyl atoms and neighboring α-carbons (r.m.s.d. of the fitted C8, C9, C10 and O1 atoms is 0.0120 Å in 1 and 0.0030 Å in 3). Their C10—C11—C12—C13 and C10—C11—C12—C17 torsion angles are likewise similar (Table 2). In the chalcones derived from β-ionone, the molecular skeleton is not so bent as in those made up of α-ionone. These corresponding mean planes are bent by 70(2)° and 44 (3)° in the major and minor populations of 2 (r.m.s.d. of the fitted C8, C9, C10 and O1 atoms is 0.0045), by 52.93(8)° in 4 (r.m.s.d. of the fitted C8, C9, C10 and O1 atoms is 0.0144), by 5.39(15) in both major and minor populations of 5 (r.m.s.d. of the fitted C8, C9, C10 and O1 atoms is 0.0014), by 36.50(18)° and 36.52(19)° in the equally distributed populations of 6 (r.m.s.d. of the fitted C8, C9, C10 and O1 atoms is 0.0151), by 37.9(2) in both major and minor populations of 7 (r.m.s.d. of the fitted C8, C9, C10 and O1 atoms is

Table 1 Crystal data and refinement statistics for the terpenoid-like chalcones prepared in this study.

		1	3	4	5	6	7	8
Structural formula		$C_{20}H_{23}N_1O_3$	$C_{20}H_{23}N_1O_3$	$C_{20}H_{23}N_1O_3$	$C_{20}H_{23}N_1O_3$	$C_{20}H_{23}Br_1O_1$	$C_{20}H_{23}Cl_1O_1$	$C_{21}H_{26}O_1$
fw (g/mol)		325.39	325.39	325.39	325.39	359.29	314.83	294.42
Cryst dimensions (mm^3)		0.30 × 0.15 × 0.05	0.20 × 0.12 × 0.05	0.30 × 0.10 × 0.07	0.24 × 0.11 × 0.010	0.26 × 0.14 × 0.06	0.32 × 0.10 × 0.08	0.20 × 0.11 × 0.08
Cryst syst		Monoclinic	Monoclinic	Orthorhombic	Monoclinic	Monoclinic	Monoclinic	Orthorhombic
Space group		$P2_1/c$	$P2_1/c$	*Pbca*	$P2_1/n$	$P2_1$	$P2_1$	*Pbca*
Z/Z'		4/1	4/1	8/1	4/1	2/1	2/1	8/1
T (K)		296(2)	296(2)	296(2)	296(2)	296(2)	296(2)	296(2)
Unit cell dimensions	a (Å)	11.861(2)	11.795(4)	15.0889(2)	7.2965(3)	8.0330(17)	7.9898(17)	15.205(2)
	b (Å)	14.277(2)	14.264(5)	10.65460(10)	19.3388(7)	10.228(2)	10.2912(17)	10.8720(15)
	c (Å)	10.9753(18)	11.053(4)	22.1010(3)	12.7689(5)	11.254(2)	11.196(3)	22.373(2)
	α (°)	90	90	90	90	90	90	90
	β (°)	97.551(2)	93.151(10)	90	92.895(3)	106.71(2)	106.966(10)	90
	γ (°)	90	90	90	90	90	90	90
V ($Å^3$)		1842.3(5)	1856.9(10)	3553.09(8)	1799.46(12)	885.6(3)	880.5(3)	3698.5(8)
Calculated density (Mg/m^3)		1.173	1.164	1.217	1.201	1.347	1.187	1.058
Absorption coefficient μ (mm^{-1})		0.078	0.078	0.081	0.080	2.321	0.217	0.063
θ range for data collection (°)		3.34–25.74	2.33–26.62	1.84–26.45	1.91–25.24	2.65–25.70	2.67–25.64	1.82–25.35
Index ranges	h	−12 to 14	−14 to 14	−18 to 15	−8 to 8	−9 to 9	−9 to 9	−18 to 17
	k	−17 to 14	−15 to 16	−13 to 10	−23 to 23	−7 to 12	−12 to 8	−13 to 13
	l	−13 to 5	−13 to 10	−27 to 27	−14 to 15	−10 to 13	−13 to 12	−24 to 26
Data collected		7143	8991	26,159	12,033	4793	4218	22,665
Unique reflections		3477	3562	3654	3228	2566	2357	3368
Symmetry factor (R_{int})		0.0252	0.0244	0.0236	0.0333	0.0227	0.0197	0.0741
Completeness to θ_{max} (%)		98.6	94.9 (to 25°)	99.7	99.2	97.5	98.2	99.6
$F(000)$		696	696	1392	696	372	336	1280
Parameters refined		220	220	220	247	229	229	226
Goodness-of-fit on F^2		1.159	1.037	1.061	1.050	1.054	1.031	1.082
Final $R1$ factor for $I > 2\sigma(I)$		0.1003	0.0816	0.0515	0.0504	0.0264	0.0364	0.0704
w$R2$ factor for all data		0.3421	0.2757	0.1623	0.1487	0.0678	0.0942	0.2637
Largest diff. peak/hole ($e/Å^3$)		0.611/−0.350	0.899/−0.307	0.347/−0.226	0.184/−0.171	0.410/−0.317	0.114/−0.146	0.247/−0.247
CCDC deposit number		1029766	1029767	1029768	1029769	1029770	1029771	1029772

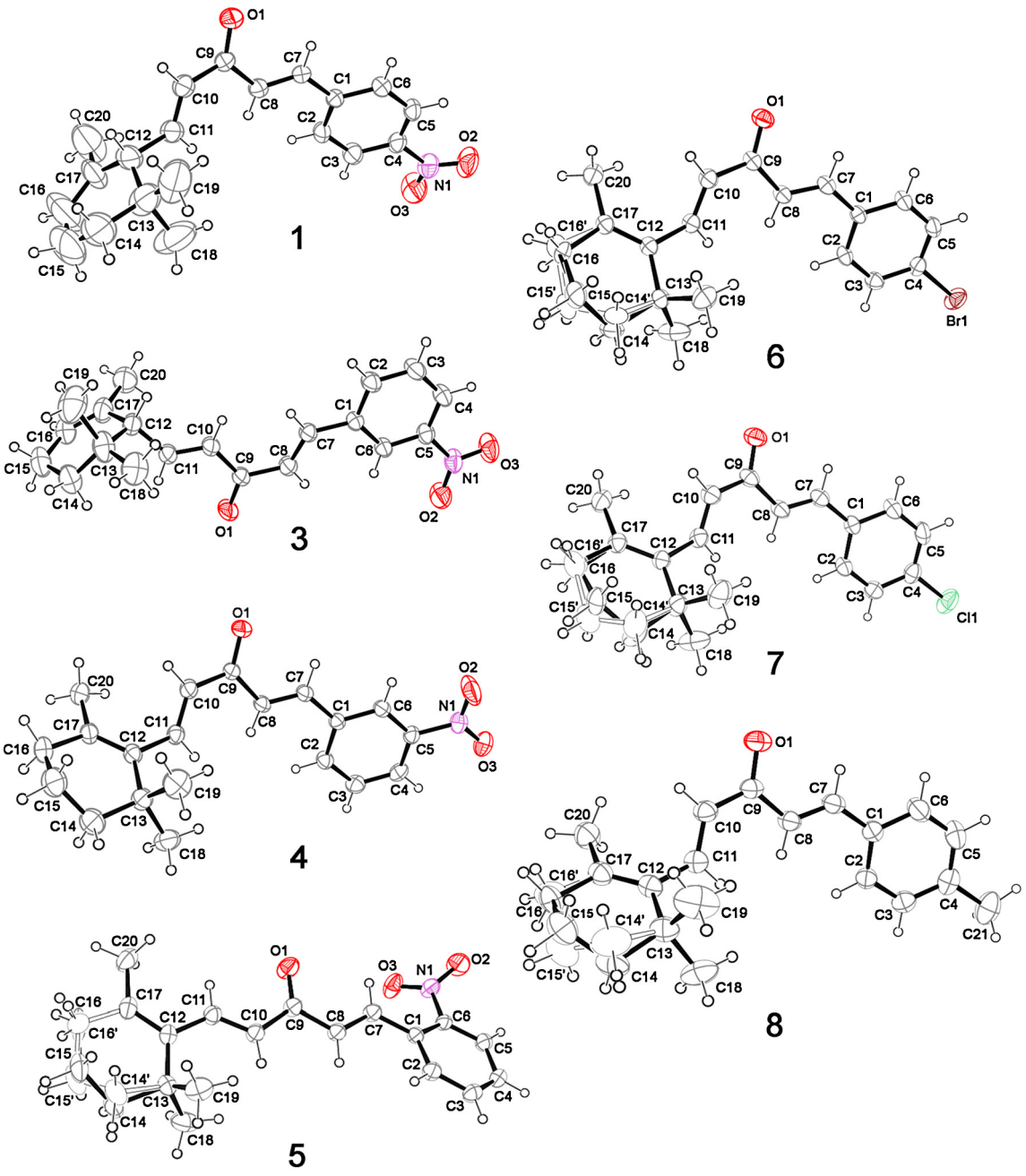

Figure 1 Asymmetric units of terpenoid-like chalcones crystallographically elucidated in this study. Non-hydrogen atoms are represented as 30% probability ellipsoids, while hydrogens are shown as arbitrary radius spheres. Ellipsoids of the carbon fractions in disordered positions of minor occupancy (or equal occupancy in 6) are drawn as boundaries, and open lines draw bonds between these atom fractions.

0.0258), and by 58.6(2)° in both major and minor populations of 8 (r.m.s.d. of the fitted C8, C9, C10 and O1 atoms is 0.0126).

As can be viewed in Table 2, the C10—C11—C12—C13 torsion angle of the β-ionone derived chalcones (except 5) is larger than the corresponding ones of 1 and 3 whereas in turn their C10—C11—C12—C17 torsion is lower than those of 1 and 3. This reflects the fact that cyclohexene ring is less bent in β-ionone-type compounds than in α-ionone derived chalcones present with cyclohexene ring almost perpendicular to the core molecular plane. This high planarity of β-ionone chalcones is highlighted in compound 5. Besides its lowest angle value between the carbonyl/α-carbons and cyclohexene mean planes, its C10—C11—C12—C13 and C10—C11—C12—C17 torsion angles are close to 0° and 180°, respectively (Table 2).

The central mean plane formed with carbonyl atoms and α-carbons and the substituted aromatic ring are not much bent in all terpenoid-like chalcones, forming angles between them of 37.53(14)°, 13.49(13)°, 2.59(12)°, 31.40(7)°, 22.46(9)°, 26.64 (9)°, 25.33(11)°, and 21.0(11)° in 1–8, respectively. The torsions around the C1—C7 bond axis are also near to either 0° (torsion

Table 2 Selected dihedral angles (°) for terpenoid-like chalcones 1–8.

Structure part	Torsion	1	2[a]	3	4	5[a]	6	7	8
Cyclohexene ring	C12—C13—C14—C15	55.6(9)	19.2(14)/−37.0(14)[b]	−50.6(5)	−39.6(2)	−50.3(6)/53.3(7)	−42.2(11)/49.1(10)	−50.9(14)/40.6(12)	48.6(18)/−45.9(10)
	C13—C14—C15—C16	−36.2(14)	−43.8(16)/44.4(17)	35.5(5)	60.3(3)	68.8(8)/−70.7(10)	61.8(14)/−70.6(14)	69.2(16)/−62.3(15)	−69(2)/64.1(13)
	C14—C15—C16—C17	11.9(18)	39.5(17)/−29.0(14)	−17.6(5)	−46.2(3)	−52.4(11)/51.5(13)	−54(2)/49.6(18)	−55.5(19)/48.4(17)	53(2)/−48.8(16)
	C15—C16—C17—C12	−8.5(16)	−16.5(19)/13.0(16)	14.7(6)	15.5(3)	15.7(14)/−16.6(13)	23(2)/−17(2)	25(2)/−18.0(17)	−22(2)/17.3(16)
	C16—C17—C12—C13	28.2(9)	−6(2)/−7(2)	−26.9(5)	4.4(3)	1.2(8)/−0.2(7)	−0.6(11)/−0.1(13)	−1.1(12)/1.0(11)	2.7(17)/0.9(9)
	C17—C12—C13—C14	−48.5(7)	5.6(17)/19.0(19)	43.8(4)	7.2(3)	16.1(4)/−17.3(4)	11.2(7)/−12.7(6)	14.9(9)/−9.6(7)	−15.8(11)/12.7(7)
C11—C12 bridge	C10—C11—C12—C13	−116.8(5)	132.9(8)/−17(2)	−121.0(3)	−130.22(19)	2.0(4)	−134.1(3)	−132.0(3)	−126.1(3)
	C10—C11—C12—C17	116.9(5)	−51.4(18)/156.8(9)	115.4(3)	47.8(3)	−177.0(2)	45.1(4)	46.8(5)	53.5(5)
C1—C7 bridge	C2—C1—C7—C8	15.8(5)	2.5(4)	175.5(2)	11.4(2)	−26.7(4)	3.8(4)	4.9(5)	9.1(5)
	C6—C1—C7—C8	−164.1(3)	−179.0(2)	−3.7(4)	−167.11(17)	156.0(2)	−175.5(3)	−174.2(3)	−170.0(3)
C8—C9 and	C8—C9—C10—C11	−2.2(5)	155.6(3)	178.85(2)	5.7(3)	−176.6(2)	−6.7(4)	−8.5(5)	7.3(5)
C9—C10 single bonds	O1—C9—C10—C11	179.7(3)	−23.6(4)	−0.67(4)	−171.92(17)	3.2(3)	175.6(3)	175.6(3)	−170.5(3)
	O1—C9—C8—C7	21.3(5)	11.8(4)	−173.78(3)	18.6(2)	2.6(3)	19.7(4)	18.5(5)	10.8(4)
	C7—C8—C9—C10	−156.7(3)	167.4(3)	6.68(4)	−158.94(16)	−177.6(2)	−157.7(3)	−157.2(3)	−167.1(3)

[a] Compounds 2 and 5 have been previously synthesized and featured (Zou et al., 2012; Fernandes et al., 2013), even though crystal data of 5 are from our structure redetermination.

[b] When two values are shown for a same torsion, they refer to conformations in the major and minor occupancy sites, in that order, except for compound 6 in which both conformations are equally distributed over the crystal lattice.

C2—C1—C7—C8) or 180° (torsion C6—C1—C7—C8) in terpenoid-like chalcones 1, 2, 4–8 and therefore reinforce the coplanarity feature between aromatic ring and the α,β-unsaturated carbonyl moiety. In terpenoid-like chalcone 3, the torsion C6—C1—C7—C8 is close to 0° while the torsion C2—C1—C7—C8 is near to 180°. This indicates that such coplanarity does also occur in this compound but it is present with a rotation of ca. 180° about the C8—C9 bond axis relative to all other terpenoid-like chalcones studied here (Fig. 2). The torsions around this bond measure near to 180° (O1—C9—C8—C7) or 0° (C7—C8—C9—C10) in 3, while there is inversion of their values in all other terpenoid-like chalcones, i.e., O1—C9—C8—C7 and C7—C8—C9—C10 are close to 0° and 180°, respectively (Table 2). Likewise, the torsions on the C9—C10 bond are similar in 2, 3 and 5, but their values are changed by ca. 180° in the other terpenoid-like chalcones (Table 2). Therefore, a twofold rotation on the C9—C10 bond axis can be also described for these compounds when compared to terpenoid-like chalcones 1, 4, 6–8 (Fig. 2). It is also noticeable the high coplanarity between aromatic ring and the α,β-unsaturated carbonyl moiety in compound 3 due to the negligible value of the angle between their least-square planes.

Nitro group is noticeably twisted only in compound 5, with its plane forming an angle of 38.41(7)° with the phenyl mean plane. In all other nitro-substituted terpenoid-like chalcones, these two moieties are considerably coplanar with angles between them of 12.9(4)°, 7.3(3)°, 7.8(3)°, and 4.82(17)° in 1–4, respectively. In addition, inspection of bond lengths indicates that electron delocalization does not encompass the molecule backbone of all chalcones (Table 3). Bond lengths of the α,β-unsaturated carbonyl moiety and of the bridges between this moiety and six-membered rings are in good agreement with expected values for pure single and double bonds.

3.2. Cytotoxic activity

All synthesized terpenoid-like-chalcones were evaluated for their *in vitro* cytotoxic activity against three human cancer cell lines (SF-295, HCT-116 and OVCAR-8). The antiproliferative activity assay results are shown in Tables 4 and 5.

As can be viewed in Table 4, terpenoid-like chalcones have almost entirely inhibited all cancer cell lines tested, except for compounds 4 and 6 inhibiting ca. 60% the SF-295 cell line and compound 5 inhibiting also ca. 60% the HCT-116 cell line. Therefore, a very broad spectrum of antiproliferative effects was observed for all compounds. In concentration of 50 μg/ml, the compounds displayed significant antiproliferative effects against SF-295, HCT-116 and OVCAR-8 cell lines. The relative potency of cell growth inhibition is shown in Table 5 in which as low the IC_{50} value of a terpenoid-like chalcone as high its cytotoxic activity. It is noteworthy that compounds 1 and 5 possess antiproliferative effect against HCT-116 cells. In fact, compounds 1 and 2, both of them with *para*-nitro moiety and derived from α- and β-ionone, respectively, and compound 3, with *meta*-nitro group and derived from α-ionone, and compound 5, with *ortho*-nitro group and derived from β-ionone, were notably the most active terpenoid-like chalcones among all those tested. Their IC_{50} values range from 2.88 to 10.84 μmol/L (compound 1), from 3.99 to 10.26 μmol/L (compound 2), from 4.33 to 6.20 μmol/

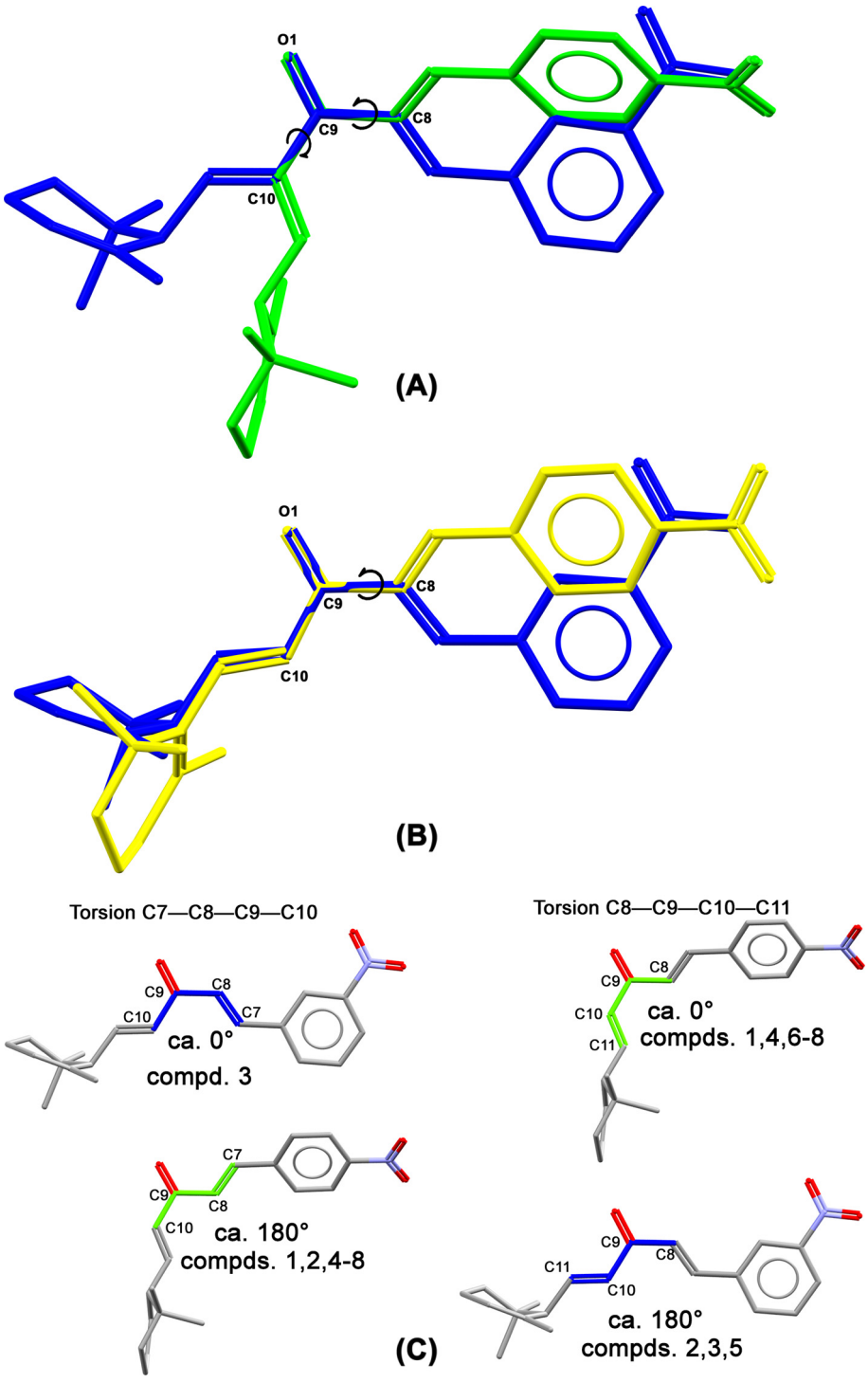

Figure 2 Molecular overlay through carbonyl atoms and neighboring α-carbons of (A) compounds 1 (green) and 3 (blue); and (B) compounds 2 (yellow) and 3 (blue). The 180° rotations on the C8—C9 and C9—C10 bond axes converting one molecule conformation into another one are highlighted (circular arrows). (C) Selected torsions describing the conformations around C8—C9 and C9—C10 bonds found in the chalcone derivatives studied here.

L (compound 3), and from 2.70 to 8.85 μmol/L (compound 5). Compound 4 with *meta*-nitro group and derived from β-ionone was slightly less active than all other nitro-substituted analogs (IC_{50} ranging from 5.22 to 20.28 μmol/L). This reveals the presence of one nitro moiety at any position of aromatic ring is decisive for antiproliferative activity of the terpenoid-like chalcones, whereas cyclohexene type does not affect much cytotoxic activity. Against other cancer lines, such as prostate (PC-3), breast (MCF), central nervous system (IMR32), and cervix (HeLa), the presence of one nitro group at *para* position of phenyl increases much the cytotoxicity of the β-ionone derived chalcone 2a (Sharma

Table 3 Selected bond lengths (Å) for terpenoid-like chalcones 1–8.

Bond	1	2[a]	3	4	5[a]	6	7	8
O1—C9	1.225(4)	1.228(3)	1.221(3)	1.225(2)	1.224(3)	1.219(4)	1.230(4)	1.236(4)
C1—C7	1.466(4)	1.461(4)	1.468(3)	1.467(2)	1.467(3)	1.458(4)	1.465(4)	1.463(4)
C7—C8	1.316(4)	1.314(4)	1.307(3)	1.318(2)	1.321(3)	1.315(4)	1.314(4)	1.318(4)
C8—C9	1.480(4)	1.474(4)	1.475(4)	1.477(2)	1.477(3)	1.471(4)	1.469(4)	1.471(4)
C9—C10	1.454(5)	1.459(4)	1.464(4)	1.463(2)	1.467(3)	1.477(4)	1.471(4)	1.459(4)
C10—C11	1.306(4)	1.323(4)	1.307(4)	1.322(3)	1.326(3)	1.319(4)	1.311(4)	1.319(4)
C11—C12	1.485(6)	1.496(16)	1.496(4)	1.471(2)	1.455(3)	1.478(4)	1.482(4)	1.468(4)

[a] Compounds 2 and 5 have been previously synthesized and featured (Zou et al., 2012; Fernandes et al., 2013), even though crystal data of 5 are from our structure redetermination.

Table 4 Cytotoxicity of terpenoid-like chalcones against three tumor cell lines.[a,b]

Compound	SF-295	HTC-116	OVCAR-8
1	99.09 ± 1.40	100 ± 0.58	99.93 ± 0.28
2	99.21 ± 0.00	99.54 ± 0.51	99.41 ± 0.64
3	99.53 ± 0.22	98.46 ± 0.15	97.85 ± 1.01
4	62.29 ± 5.87	99.59 ± 0.58	98.50 ± 0.83
5	99.25 ± 0.50	59.44 ± 0.00	95.97 ±4.05
6	60.75 ± 4.61	100 ± 0.58	99.80 ± 1.93
7	98.42 ± 0.56	96.35 ± 1.09	94.53 ± 4.60
8	97.98 ± 1.62	99.38 ± 0.58	98.76 ± 0.83
Dexorrubicin[c]	97.40 ± 0.10	98.55 ± 0.13	99.00 ± 0.10

[a] Cancer cell lines: SF-295, central nervous system. HTC-116, colon cancer and OVCAR-8, breast cancer.
[b] Cell-growth inhibition percentage (GI-%) was measured at a compound concentration of 25 μg/mL and is shown as the average of three replicates followed by standard deviation.
[c] Positive control at 5 μg/mL.

et al., 2013), which did also occur in another chalcone with two phenyl moieties (bearing three methoxy groups in the B-ring and one para-nitro group in the A-ring) (Bandgar et al., 2010). The presence of nitro moiety in the 2-position of phenyl rings has been likewise responsible to improve the anticancer activity of curcumin related compounds similar to chalcones (Bukhari et al., 2014a).

The inspection of IC_{50} values does also show another interesting structure–activity relationship. There is a trend of decrease in cytotoxic activity with weak electron-withdrawing groups at phenyl ring. This has been reported previously for anticancer (Singh et al., 2014; Bandgar et al., 2010) and anti-inflammatory properties of chalcones (Bukhari et al., 2012). More precisely, the presence and strength of electron withdrawing groups in the phenyl ring of β-ionone derived chalcones have been found to be decisive for their cytotoxicity (Sharma et al., 2013) as well as in methoxychalcones (Singh et al., 2014; Bandgar et al., 2010). In agreement with these previous findings, the presence of either bromine or chlorine, which are less electron-withdrawing than nitro moiety, at *para*-position does decreases cytotoxic activity of terpenoid-like chalcones 6 and 7 (IC_{50} ranging from 12.55 to 19.28 μmol/L for compound 6 and from 9.27 to 22.61 μmol/L for compound 7) relative to nitro derivatives 1 and 2. Similar IC_{50} values have been found for related halogenated chalcones bearing two phenyl moieties bonded at 1,3-positions of prop-2-en-1-one (Dias et al., 2013). Chalcones with *ortho*-hydroxyphenyl group bonded to carbonyl carbon and one either *meta* or *para* halogenated (F, Cl or Br) phenyl ring bonded to β-carbon have shown IC_{50} values in the 10.9–20.9 μmol/L range against colorectal carcinoma cell line HCT-116 (Dias et al., 2013). Also, *ortho*-hydroxychalcones with halogen substitution at *para* position were less active than those halogenated at *meta* position. Against the same cell line HCT-116, *para*-halogenated *ortho*-hydroxychalcones with Br and Cl had similar IC_{50} values of 19.1 and 20.9 μmol/L (Dias et al., 2013), whereas these average values for our related compounds 6 and 7 were 19.23 and 9.27 μmol/L. This indicates that β-ionone and a further α,β-unsaturated set of carbons can increase anticancer activity from Br to Cl. Similar trend of increasing cytotoxicity as halogen substitution in the *ortho*-position of the phenyl ring bonded to β-carbon goes from Br

Table 5 IC_{50} values of terpenoid-like chalcones against three cancer cell lines.[a,b]

Compound	SF-295	HTC-116	OVCAR-8
1	10.84 (8.94–13.15)	2.88 (2.27–3.68)	6.33 (5.32–7.49)
2	3.99 (2.79–5.74)	10.26 (8.75–12.05)	4.39 (3.96–4.85)
3	6.20 (4.54–8.45)	4.48 (3.50–5.71)	4.33 (3.78–4.97)
4	20.28 (13.58–30.30)	5.22 (4.91–5.56)	7.19 (6.20–8.17)
5	8.85 (6.64–11.83)	2.70 (2.21–3.26)	6.36 (5.62–7.19)
6	19.28 (13.91–26.69)	19.23 (14.44–26.60)	12.55 (10.60–14.86)
7	22.61 (19.63–26.11)	9.27 (7.46–11.53)	12.64 (10.83–14.71)
8	35.39 (32.19–38.85)	15.86 (11.37–22.08)	32.19 (28.49–36.37)
Doxorrubicin[c]	0.44 (0.37–0.49)	0.22 (0.17–0.31)	0.48 (0.31–0.55)

[a] Cancer cell lines: SF-295, central nervous system. HTC-116, colon cancer and OVCAR-8, breast cancer.
[b] IC_{50} (CI 95%) [μmol/L]: 50% inhibitory concentration and 95% confidence interval.
[c] Positive control.

to F was also observed in chalcones with 1,3-diphenyl moieties against a colon cell line (COLO-205) (Jain et al., 2014). Such an increasing was followed by the increase in the lipophilicity of the substituent in the *para*-position of phenyl ring bonded to carbonyl carbon from methoxy to phenoxy (Jain et al., 2014). When compared with the cytotoxic profile of compounds 6 and 7 against a colorectal cell line, it appears that this biological activity of chalcones increases as the lipophilicity of the moiety neighbor to carbonyl and as electron-withdrawing strength of one halogen in the phenyl ring attached at the other tail of prop-2-en-1-one, regardless of its position.

In our compounds, antiproliferative effect reduction is still highlighted in compound 8 present with *para*-methyl moiety (IC_{50} ranging from 15.86 to 35.39 μmol/L). Indeed, this last compound was the less active terpenoid-like chalcone against all cancer cell lines.

Several articles show the anticancer potential of chalcones and their derivatives with selectivity for cancer cells, demonstrating the therapeutic potential of this chemical class (Jandial et al., 2014). Champelovier et al. (2013) showed selectivity of two chalcones (A and B) for the LN229 lineage (glioblastoma tumor cells) relative to the mononuclear cells from peripheral blood and skin fibroblasts. Both chalcones were able to cause intracellular oxidative stress, accumulation of cells in G2/M, besides chalcone A activating the caspase apoptotic pathway and chalcone B inducing cell death by autophagy without affecting proliferation of normal cells.

Tang et al. (2010) also showed that the compound flavokawain B, the chalcone kava, was effective in reducing the viability of cell lines DU145, PC3, LAPC4 and LNCaP, all strains of prostate cancer, with minimal cytotoxicity against normal cells from prostate epithelium and stroma. In cancer cells, this chalcone induces apoptosis by increasing the expression of pro-apoptotic proteins such as death receptor-5, Bim and Puma and by decreasing the expression of the apoptosis inhibitors such as XIAP and survivin.

In another work, the series of boronic-chalcone derivatives were synthesized and shown to be effective in inhibiting the proliferation of breast cancer cells at micromolar concentrations (MDA-MB-435, MDA-MB-231, Wt, MCF7), without affecting the viability and proliferation of normal mammary epithelial cells, MCF-10A and MCF-12A (Kumar et al., 2003). Furthermore, it was shown that indanocine, a chalcone-like compound, is an antimitotic and cytotoxic compound that blocks the polymerization of tubulin, inducing cell death by apoptosis in cancer cells resistant to multiple drugs at concentrations that are non-cytotoxic to non-carcinogenic cells (Leoni et al., 2000).

These literature data therefore reveal that besides synthetic chalcones having anticancer potential, many compounds of this class exhibit selectivity for tumor cells, which allow us to believe that the compounds reported in this study can also show selectivity for the cancer cells such as SF-295, HCT-116 and OVCAR-8 assessed here. So we can infer that the compounds derived from chalcones, as terpenoid-like chalcones, are promising for the development of new drugs to fight cancer.

4. Conclusions

Eight compounds with both ionone and chalcone cores were synthesized in this study. The Claisen–Schmidt condensation was employed using either α- or β-ionone and substituted benzaldehydes. The structures of six compounds were elucidated by single-crystal X-ray diffraction technique for the first time. Detailed crystal structure inspection, including the analysis of other related terpenoid-like chalcones whose structures are already reported in the literature, has revealed interesting conformational features such as cyclohexene ring adopting half-chair conformation with C13 at the flap only in α-ionone type chalcones. On the other hand, twist puckering of cyclohexene with C14 and C15 deviating from the other coplanar carbons is commonly found in β-ionone chalcones including conformerism featured by the flipping of these carbons in a same structure. Furthermore, α-ionone derived chalcones are present with cyclohexene ring almost perpendicular to the α,β-unsaturated carbonyl mean plane, while the last plane and the substituted aromatic ring are not much bent in all terpenoid-like chalcones. There is also a rotation of ca. 180° about the C8—C9 bond axis of the α-ionone-type chalcone with nitro moiety at *meta*-position of phenyl if all other terpenoid-like chalcones studied here were taken as references. Likewise, terpenoid-like chalcones can also adopt two different conformations due to a 180° rotation on the C9—C10 bond axis.

All compounds synthesized in this study and another related terpenoid-like chalcone were also evaluated for their cytotoxic activity against three cancer cell lines (SF-295, HCT-116 and OVCAR-8), being observed a very broad spectrum of antiproliferative effects. Moreover, compounds with nitro group in phenyl, regardless of its position, and derived from either α- or β-ionone were the most active terpenoid-like chalcones among all those tested, revealing that the presence of one nitro moiety is decisive for cytotoxicity of the terpenoid-like chalcones whereas cyclohexene type does not affect much this biological property. The tendency of decrease in cytotoxic activity with weak electron-withdrawing groups at phenyl ring was also supported on the basis of IC_{50} values.

Acknowledgments

We thank the Brazilian Research Council CNPq (Conselho Nacional de Desenvolvimento Científico e Tecnológico) for the financial support (Processos 472623/2011-7 and 478336/2013-2). F.T.M. also thanks the CNPq for research fellowship. C.C.S also thanks FAPEG (Fundação de Amparo à Pesquisa do Estado de Goiás) for the scholarship (Processo 201410267000635).

References

Asiri, A.M., Khan, S.A., 2011. Synthesis and anti-bacterial activities of a bis-chalcone derived from thiophene and its bis-cyclized products. Molecules 16, 523–531.

Bandgar, B.P., Gawande, S.S., Bodade, R.G., Totre, J.V., Khobragade, C.N., 2010. Synthesis and biological evaluation of simple methoxylated chalcones as anticancer, anti-inflammatory and antioxidant agents. Bioorg. Med. Chem. 18, 1364–1370.

Berridge, M.V., Tan, A.S., Mccoy, K.D., Wang, R., 1996. The biochemical and cellular basis of cell proliferation assays that use tetrazolium salts. Biochemica 4, 14–19.

Bruker, 2012. SAINT. Program for Data Reduction from Area Detectors. BRUKER AXS Inc., 5465 East Cheryl Parkway, Madison, WI 53711-5373, USA.

Bukhari, S.N.A., Franzblau, S.G., Jantan, I., Jasamai, M., 2013a. Current prospects of synthetic curcumin analogs and chalcone derivatives against *Mycobacterium tuberculosis*. Med. Chem. 9, 897–903.

Bukhari, S.N.A., Jantan, I., Jasamai, M., 2013b. Anti-Inflammatory trends of 1,3-diphenyl-2-propen-1-one derivatives. Mini Rev. Med. Chem. 13, 87–94.

Bukhari, S.N.A., Jantan, I., Tan, O.U., Sher, M., Naeem-ul-Hassan, M., Qin, H.-L., 2014a. Biological activity and molecular docking

studies of curcumin-related α, β-unsaturated carbonyl-based synthetic compounds as anticancer agents and mushroom tyrosinase inhibitors. J. Agric. Food Chem. 62, 5538–5547.
Bukhari, S.N.A., Jasamai, M., Jantan, I., 2012. Synthesis and biological evaluation of chalcone derivatives (mini review). Mini Rev. Med. Chem. 12, 1394–1403.
Bukhari, S.N.A., Lauro, G., Jantan, I., Bifulco, G., Amjad, M.W., 2014b. Pharmacological evaluation and docking studies of α, β-unsaturated carbonyl based synthetic compounds as inhibitors of secretory phospholipase A2, cyclooxygenases, lipoxygenase and proinflammatory cytokines. Bioorg. Med. Chem. 22, 4151–4161.
Bukhari, S.N.A., Tajuddin, Y., Benedict, V.J., Lam, K.W., Jantan, I., Jalil, J., Jasamai, M., 2014c. Synthesis and evaluation of chalcone derivatives as inhibitors of neutrophils' chemotaxis, phagocytosis and production of reactive oxygen species. Chem. Biol. Drug Des. 83, 198–206.
Bukhari, S.N.A., Zhang, X., Jantan, I., Zhu, H.-L., Amjad, M.W., Masand, V.H., 2015. Synthesis, molecular modeling, and biological evaluation of novel 1, 3-diphenyl-2-propen-1-one based pyrazolines as anti-inflammatory agents. Chem. Biol. Drug Des. 85, 729–742.
Burla, M.C., Caliandro, R., Camalli, M., Carrozzini, B., Cascarano, G.L., De Caro, L., Giacovazzo, C., Polidori, G., Spagna, R., 2005. SIR2004: an improved tool for crystal structure determination and refinement. J. Appl. Cryst. 38, 381–388.
Champelovier, P., Chauchet, X., Hazane-Puch, F., Vergnaud, S., Garrel, C., Laporte, F., Boutonnat, J., Boumendjel, A., 2013. Cellular and molecular mechanisms activating the cell death processes by chalcones: critical structural effects. Toxicol. In Vitro 27, 2305–2315.
Chandra, N., Pandey, S., Suryawanshi, S.N., Gupta, S., 2006. Chemotherapy of leishmaniasis, part VII: Synthesis and bioevaluation of novel aryl-substituted terpenyl pyrimidines as antileishmanial agents. Eur. J. Med. Chem. 41, 779–785.
Dias, T.A., Duarte, C.L., Lima, C.F., Proença, M.F., Pereira-Wilson, C., 2013. Superior anticancer activity of halogenated chalcones and flavonols over the natural flavonol quercetin. Eur. J. Med. Chem. 65, 500–510.
Farrugia, L.J., 1997. ORTEP-3 for Windows – a version of ORTEP-III with a Graphical User Interface (GUI). J. Appl. Crystallogr. 30, 565.
Fernandes, W.B., Malaspina, L.A., Martins, F.T., Lião, L.M., Camargo, A.J., Lariucci, C., Noda-Perez, C., Napolitano, H.B., 2013. Conformational variability in a new terpenoid-like bischalcone: structure and theoretical studies. J. Struct. Chem. 54, 1112–1121.
Findik, E., Dingil, A., Karaman, I., Ceylan, M., 2009. Synthesis of terpenoid-like bischalcones from α- and β-ionones and their biological activities. Synth. Commun. 39, 4362–4374.
Jain, U.K., Bhatia, R.K., Rao, A.R., Singh, R., Saxena, A.K., Sehar, I., 2014. Design and development of halogenated chalcone derivatives as potential anticancer agents. Trop. J. Pharm. Res. 13, 73–80.
Jandial, D.D., Blair, C.A., Zhang, S., Krill, L.S., Zhang, Y.-B., Zi, X., 2014. Molecular targeted approaches to cancer therapy and prevention using chalcones. Curr. Cancer Drug Tar. 14, 181–200.
Jantan, I., Bukhari, S.N.A., Adekoya, O.A., Sylte, I., 2014. Studies of synthetic chalcone derivatives as potential inhibitors of secretory phospholipase A2, cyclooxygenases, lipoxygenase and pro-inflammatory cytokines. Drug Des. Dev. Ther. 8, 1405–1418.
Kumar, S.K., Hager, E., Pettit, C., Gurulingappa, H., Davidson, N.E., Khan, S.R., 2003. Design, synthesis, and evaluation of novel boronic-chalcone derivatives as antitumor agents. J. Med. Chem. 46, 2813–2825.
Leoni, L.M., Hamel, E., Genini, D., Shih, H.C., Carrera, C.J., Cottam, H.B., 2000. Indanocine, a microtubule-binding indanone and a selective inducer of apoptosis in multidrug-resistant cancer cells. J. Natl. Cancer Inst. 92, 217–224.
Lutz-Wall, S., Fischer, P., Schmidt-Dannert, C., Wohlleeben, W., Hauer, B., Schmid, R.D., 1998. Stereo- and regioselective hydroxylation of α-ionone by *Streptomyces* strains. Appl. Environ. Microbiol. 64, 3878–3881.
Macrae, C.F., Bruno, I.J., Chisholm, J.A., Edgington, P.R., McCabe, P., Pidcock, E., Monge, L.R., Taylor, R., van de Streek, J., Wood, P.A., 2008. Mercury CSD 2.0 – new features for the visualization and investigation of crystal structures. J. Appl. Crystallogr. 41, 466–470.
Markovich, Y.D., Panfilov, A.V., Zhirov, A.A., Kosenko, S.I., Kirsanov, A.T., 1998. New cyclization agents for the synthesis of beta-ionone from pseudoionone. Pharmaceut. Chem. J. 32, 603–605.
Modzelewska, A., Pettit, C., Achanta, G., Davidson, N.E., Huang, P., Khana, S.R., 2006. Anticancer activities of novel chalcone and bischalcone derivatives. Bioorg. Med. Chem. 14, 3491–3495.
Mossman, T., 1983. Rapid colorimetric assay for cellular growth and survival: application to proliferation and cytotoxicity assays. J. Immunol. Meth. 65, 55–63.
Raj, C.G.D., Sarojini, B.K., Bhanuprakash, V., Yogisharadhya, R., Swamy, B.E.K., Raghavendra, R., 2012. Studies on radioprotective and antiviral activities of some bischalcone derivatives. Med. Chem. Res. 21, 2671–2679.
Raynaud, C., Poteau, R., Maron, L., Jolibois, F., 2006. *Ab initio* molecular dynamics simulation of the UV absorption spectrum of β-ionone. J. Mol. Struct. Theochem. 771, 43–50.
Reddy, M.V.B., Shen, Y.C., Ohkoshi, E., Bastowd, K.F., Qianc, K., Lee, K.H., Wu, T.S., 2012. Bis-chalcone analogues as potent NO production inhibitors and as cytotoxic agents. Eur. J. Med. Chem. 47, 97–103.
Sarojini, B.K., Raj, C.G.D., Ramakrishna, M.K., Ramesh, S.R., Bharath, B.R., Manjunatha, H., 2011. In silico studies of (2E,5E)-2,5-bis(3-methoxy-4-hydroxy-benzylidene)cyclopentanone on proteins AChE and BChE involved in Alzheimer's disease and ameliorative effects on paraquat induced oxidative stress markers in *Drosophila* melanogaster. Lett. Drug Des. Discov. 8, 260–267.
Sharma, V., Chaudhary, A., Arora, S., Saxena, A.K., Ishar, M.P.S., 2013. β-Ionone derived chalcones as potent antiproliferative agents. Eur. J. Med. Chem. 69, 310–315.
Sheldrick, G.M., 2008. A short history of SHELX. Acta Crystallogr. Sect. A 64, 112–122.
Singh, P., Anand, A., Kumar, V., 2014. Recent developments in biological activities of chalcones: a mini review. Eur. J. Med. Chem. 85, 758–777.
Skehan, P., Storeng, R., Scudiero, D., Monks, A., Mcmahon, J., Vistica, D., Warren, J.T., Bodesch, H., Kenney, S., Boyd, M.R., 1990. New colorimetric cytotoxicity assay for anticancer – drug screening. J. Natl. Cancer Inst. 82, 1107–1112.
Srivastava, S., Joshi, S., Singh, A.R., Yadav, S., Saxena, A.S., Ram, V. J., Chandra, S., Saxena, J.K., 2008. Oxygenated chalcones and bischalcones as a new class of inhibitors of DNA topoisomerase II of malarial parasites. Med. Chem. Res. 17, 234–244.
Suryawanshi, S.N., Bhat, B.A., Pandey, S., Chandra, N., Gupta, S., 2007. Chemotherapy of leishmaniasis, part VII: synthesis and bioevaluation of substituted terpenyl pyrimidines. Eur. J. Med. Chem. 42, 1211–1217.
Tang, Y., Li, X., Liu, Z., Simoneau, A.R., Xie, J., Zi, X., 2010. Flavokawain B, a kava chalcone, induces apoptosis via up-regulation of death-receptor 5 and Bim expression in androgen receptor negative, hormonal refractory prostate cancer cell lines and reduces tumor growth. Int. J. Cancer 127, 1758–1768.
Wang, H.K., Natschke, L.M., Lee, K.H., 1997. Recent advances in discovery and development of topoisomerase inhibitors as antitumor agents. Med. Res. Rev. 17, 367–425.
Zou, P., Jin, Y.-J., Xiang, L.-F., Sun, D.-P., Yang, S.-L., 2012. (1E,4E)-1-(2-Nitrophenyl)-5-(2,6,6-trimethylcyclohex-1-en-1-yl) penta-1,4-dien-3-one. Acta Crystallogr. Sect. E 68, o1858.